We thank the reviewer for reviewing our manuscript and providing comments to improve our work. Below are the point-by-point comments, replies and changes.

(1) Extent to which the chosen interval represents flow at the AWAKEN site and more generally. Source of data should be given (line 54). The paper identifies use of location A1 and of 08 June 2023 only with the justification that the vertical extent of the gravity wave spans the rotor layer of the wind farm. It would help the reader to show how often these types of condition occur at the AWAKEN site - if only very rarely then is this relevant for design?, if regularly then what range of AGW vertical extents occur? were similar observations (phase lagged) obtained at down-wind sites (e.g. H on Figure 1 map) or does vertical extent differ over the streamwise spacing between turbine rows? More generally atmospheric gravity waves can occur at other sites and locations so some discussion on how the conditions represent AGW conditions at wind farm sites more generally (e.g. in terms of ABL thickness and AGW wavelength - mentioned to be 2 km in LES (line 176), compared to 2.5-3 km measured (line 58)? - and amplitude, not only site roughness which is not the only important factor between sites).

### **Reply**

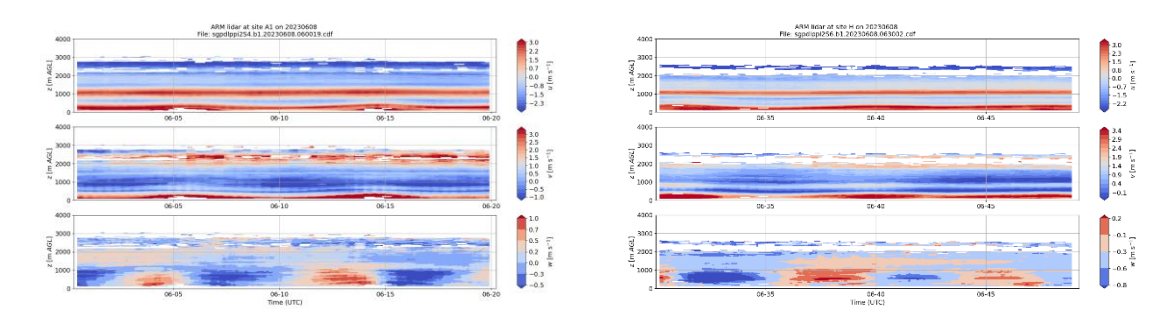
We thank the reviewer for raising questions that are crucial for clarifying both the motivation and the limitations of our work.

# (i) Source of measurement data

The AGW event analyzed in this study was first identified from horizontal scans obtained by X-band radars (shown in Fig. 2, rearranged as the right panel of Fig. 1 in the revised manuscript). The detailed wind field of AGWs was then measured using a scanning Doppler lidar located at site A1. The top-left panel of Fig. 3 (renumbered as Fig. 2 in the revised manuscript) shows the time-height history of wind speed with a temporal resolution of ~6 s and vertical spacing of ~10 m. These high-resolution measurements are assimilated to capture the transient features of AGWs.

# (ii) AGW observations at the AWAKEN site

In June 2023, four AGW events with similar wave periods of approximately 600 s were observed. Their vertical extent ranged from the surface up to ~3 km above ground level. R-Fig. 1 shows the time-height evolution of the three velocity components for the June 8 event, which is the focus of our study. In the vertical velocity component, similar large-scale wavy oscillations are observed at site A (upstream of the wind farm) and site H (downstream). Such transient atmospheric phenomena represent non-idealized atmospheric conditions that should be considered in wind farm design and operation. Accurate modeling of these phenomena is therefore important for real-time wind farm simulations.



R-Fig. 1: Three velocity components of AGWs at site A (left) and H (right).

### (iii) AGW wavelength

We confirm that the AGW wavelength reported in line 176 (simulation) is consistent with that mentioned in line 58 (measurement). As shown in Fig. 8, the spectral peak at St  $\approx 0.05$  corresponds to a characteristic length scale of  $\sim 20$  turbine diameters ( $\sim 2520$  m), which agrees well with the wavelength observed from the radar measurements in Fig. 2.

### (iv) Limitations of our work

We acknowledge the reviewer's point that AGWs vary in wavelength and in relation to atmospheric boundary layer (ABL) depth. This variability arises because AGWs can be triggered by multiple atmospheric processes, including frontal systems, thunderstorms, and orographic effects. We also agree that the vertical extent of AGWs may be modified by the blockage effect of wind turbine arrays, depending on the turbine spacing. Nevertheless, our study is intended as a preliminary investigation into how an observed AGW event influences single-turbine wake dynamics. Future work will extend this analysis to a wider range of atmospheric conditions and turbine layouts.

## Revison

- (i) We have corrected all descriptions on the AGW wavelengths as 'approximately 2.5 km'.
- (ii) We have added the source of AGW data in lines 54-56.

'Multiple AGW events have been identified from horizontal scanning by X-band radars and vertical profiling by scanning Doppler lidars. The high-resolution lidar measurements are used in our data assimilation for capturing transient features of AGWs.'

(iii) We have added some text concerning different sources of AGWs and the necessity for future studies of these in lines 262-264 in Conclusions section.

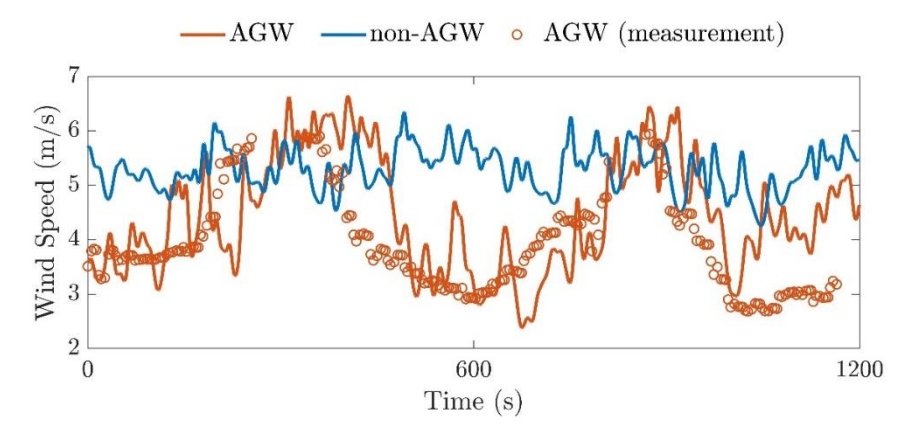
'The present work is intended as a case-study focusing on a specific AGW event. Future study should incorporate AGW events originating from various sources and with different wavelengths to comprehensively understand their roles in

### turbine wake and wind farm flows.'

(2) Extent to which the indirect profile assimilation method reproduces the LIDAR measurements of the selected AGW event. The three frames shown on left hand side of Figure 3 compare LIDAR measurements of time varying onset velocity to the simulated conditions. Lines 94-96 comment that "the present LES not only captures the low-frequency wind speed oscillations by the AGW event but also resolves turbulence structures with higher spatio-temporal resolution'. Whilst the simulation seems to capture the period of the selected AGW event there seem to be other differences that are not mentioned; for example the LES shows larger maximum velocity, possibly larger minimum velocity, change of turbulence over 0.5 < height < 1 during 06:00 to 07:00 (approx). These need to be critically assessed, particularly in the context of line 39-40 "it is unclear whether LES driven by field measurements can accurately capture transient atmospheric phenomena like AGWs". A quantitative comparison is needed of the measured and simulated conditions. Comparison of profiles - of velocity, turbulence, potential temperature - at specific time-steps during the AGW event would provide greater clarity. There should also be discussion on whether these AGW event predictions can be considered to be mesh independent and sub-grid model independent.

#### **Reply**

We agree with the reviewer that our simulation should be validated against measurement data in a more quantitative manner. In Fig. 3 (renumbered as Fig. 2 in the revised manuscript), the simulated AGW wind-speed time-height history shows good overall agreement with the AWAKEN lidar measurements. To further quantify this comparison, we have added R-Fig. 2 (Fig. 3 in the revised manuscript), which shows the hub-height wind-speed time series. The results indicate that our simulation not only captures the large-scale wavy oscillations observed in the measurements, but also resolves smaller-scale turbulence fluctuations. This detailed turbulence information provides a reliable inflow condition for turbine simulations. We did not compute spectra because the measurement data contain missing time steps and are unevenly spaced in time.



R-Fig. 2: Time series of wind speed at hub-height from simulation for both cases, AGW and non-AGW, and measurement for the AGW case, AGW (measurement).

Regarding mesh resolution and SGS model, our selections follow previous studies of idealized atmospheric boundary layers [1,2], i.e., the non-AGW case in our work. Fig. 8 in the original draft shows that the main difference between the AGW and non-AGW cases (dotted lines) is that the AGW case exhibits higher turbulent kinetic energy at relatively low frequencies, St < 1, corresponding to a characteristic length scale larger than one rotor diameter. Such large-scale turbulent fluctuations can be effectively resolved using the selected mesh resolution and SGS model.

### Revison

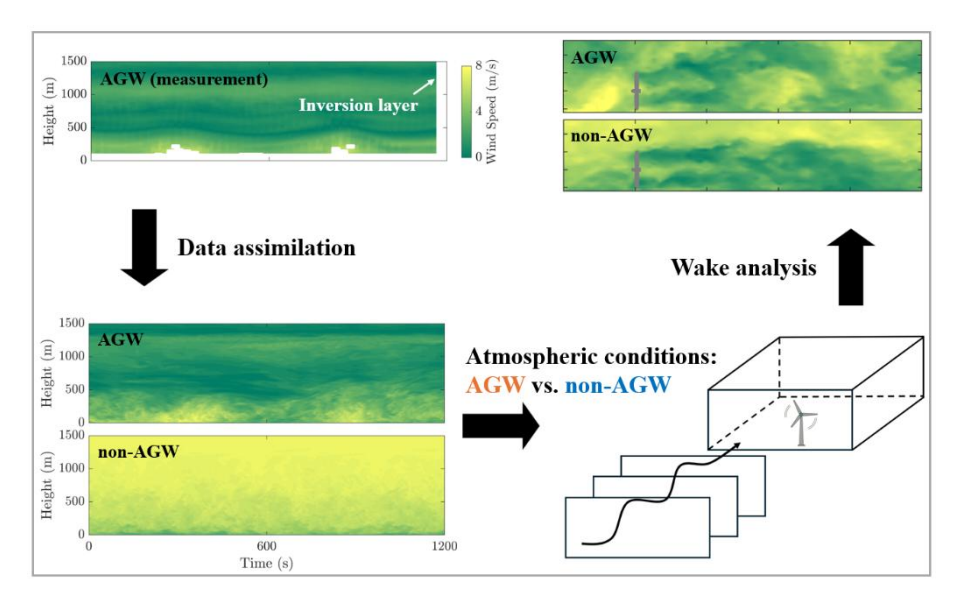
We have added Fig.3 (herein R-Fig. 2) and lines 100-102 to clarify the simulation-measurement agreement.

'To further quantify these comparisons, we show in Fig.3 wind speed time series at the hub-height. The results indicate that our simulation not only captures the large-scale wavy oscillations observed in the measurements, but also resolves smaller-scale turbulent fluctuations.'

(3) Choice of non-AGW conditions used for comparison. The same onset flow profile plots would also be useful to show the non-AGW conditions modelled rather than relying on the comments regarding similarity on lines 116-119 only. Figure 6 shows that ambient TKE is very different between the two cases so is it meaningful to compare wakes in such different turbulence conditions?

#### **Reply**

As suggested by the reviewer, we have added the time-height history of the non-AGW inflow condition to Fig. 3 (shown here as R-Fig. 3 and renumbered as Fig. 2 in the revised manuscript).



R-Fig. 3: Flow chart of the present measurement-driven LES study.

Regarding the different TKE levels, the higher TKE observed in the AGW case is expected, as the large-scale wavy oscillations contribute additional energy at relatively large characteristic length scales. The goal of our work is to examine how such transient atmospheric inflow conditions differ from the idealized atmospheric boundary layer (non-AGW case) in their influence on wake dynamics.

#### **Revison**

We have added the inflow profile for the non-AGW case in Fig. 2 (herein R-Fig. 3) and its corresponding description in lines 98-100.

'This vertical wind profile differs significantly from that for the non-AGW case, where wind speed typically increases monotonically with height above the ground.'

(4) Choice of turbine modelled. Please summarise the differences and similarities between the deployed GE 2.8 MW turbine and the NREL 5 MW reference turbine to explain why this substitution was made and highlight the implications of any differences of diameter, hub-height and operating characteristics.

#### **Reply**

Regarding the geometric features, the differences between the GE 2.8 MW turbine and the NREL 5 MW reference turbine are minor: rotor diameter of 127 m vs. 126 m, and hub height of 88.5 m vs. 90 m. For the operating condition, we simplified the rotational speed to a constant 9 rpm.

Because detailed design data of the GE 2.8 MW turbine are not publicly available, we used the NREL 5 MW reference turbine as a substitute. As our study focuses

on single-turbine wake dynamics rather than replicating the exact AWAKEN wind farm, we consider this substitution appropriate for the scope of our work.

#### **Revison**

We have added above discussions in lines 105-108.

'This open-source turbine model is used as a proxy for the 2.8-MW General Electric turbines deployed at the King Plains wind farm. Regarding the geometric features, the differences between the GE 2.8 MW turbine and the NREL 5 MW reference turbine are minor: rotor diameter of 127 m vs. 126 m, and hub height of 88.5 m vs. 90 m, respectively.'

(5) Turbine modelling approach. Reference needed for statement on line 104-105 re model choice previously demonstrating good agreement. Since the focus of this study is on locations up to 8D downstream (and for Figures 8 and 12 at 4D downstream) please clarify that the previous demonstration of good agreement for far-wake predictions relates to comparable distances.

#### **Reply**

We have added references in the revised manuscript to show that, beyond three rotor diameters downstream, the present actuator-disk model is consistent with both wind-tunnel experiments [3] and actuator-line simulations [4].

## Revison

We have added the work of Wu & Porté-Agel [3] and Stevens et al. [4] as references in lines 110-112.

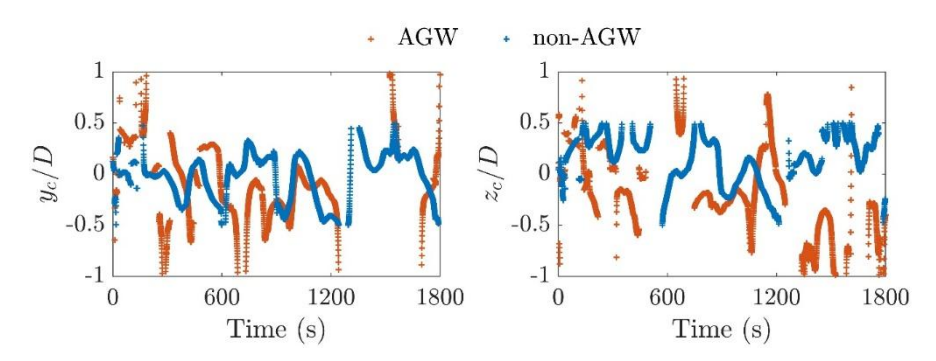
'While the effects of the nacelle and tower are neglected, this method has demonstrated good agreement with wind tunnel measurements and high-fidelity numerical simulations in the far wake region (Wu and Porté-Agel, 2011; Stevens et al. 2018), which primarily influences wind farm flow characteristics.'

(6) Meandering results. The analysis focuses on the streamwise increase of amplitude of meandering of the wake center. To relate the observed variations to the two mechanisms identified (lines 143-145) it would be helpful to show that this meandering of wake center is occurring at the AGW period (~10 mins as Fig 3?), and to show the turbulence length-scales (which are not currently stated in the manuscript), or corresponding time-scales, for each case.

#### **Reply**

We plot R-Fig. 4 to show the time history of the spanwise (left) and vertical (right) wake center for both AGW and non-AGW cases during the AGW event. The wake center locations are obtained using a two-dimensional Gaussian fit to the instantaneous wake profile at six rotor diameters downstream. Gaps appear at

some time steps, particularly in the AGW case, because the wake is too turbulent to be reliably fitted. In both directions, the magnitudes of wake-center deflections are clearly larger in the AGW case. In the spanwise direction (left panel), the AGW case exhibits distinct large-scale oscillations.



R-Fig. 4: Time history of spanwise (left) and vertical (right) wake centers for AGW and non-AGW cases.

Also, we note that the spectra shown in Fig. 8 can indicate the turbulence length scales: the inverse of the Strouhal number corresponds to the wavelength normalized by the rotor diameter.

#### **Revison**

(i) We have added clarification on large-scale wake center deflections in lines 143-147.

'The wake centers are determined by first filtering the instantaneous wake-deficit flow field with a spatial filter spanning three rotor diameters to isolate meandering motions. The filtered wake deficit is then fitted to a two-dimensional Gaussian profile at each downstream location, following the method described by Trujillo et al. (2011). The location of the maximum wake deficit is taken as the wake center. In both directions, the magnitudes of wake-center deflections are found to be larger for the AGW case, as evident in Fig. 4.'

(ii) We have added how Strouhal number indicates turbulence length scales in lines 177-178.

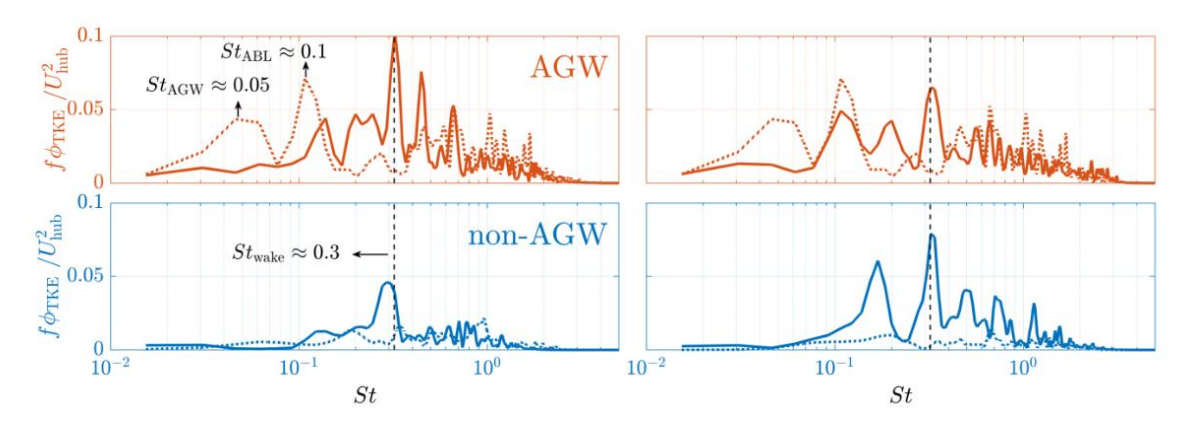
'Note that the inverse of Strouhal number corresponds to wavelength normalized by the rotor diameter, indicating the characteristic turbulence length scales.'

(7) TKE spectra analysis. This is interesting, particularly the peak sustained at Strouhal Number  $\sim 0.3$ . However, the lack of peak at St  $\sim 0.05$  in the wake in AGW case seems to indicate that there are not variations in the wake at the AGW period; does this affect line 141-142? Could the same type of spectra be shown for 8D also to better understand whether the same spectral content persists as the amplitude of meandering increases into the far wake? Is there any explanation available for the higher harmonics observed in AGW case?

#### **Reply**

We thank the reviewer for raising this important point. Lines 141–142 should be corrected to state that the enhancement of wake meandering is primarily caused by the increase in inflow turbulent kinetic energy. The explanation is as follows.

We show in R-Fig. 5 the spectra of wake (solid lines) and inflow (dashed lines) at 4D (left) and 8D (right) downstream from the single-turbine simulation. In both AGW and non-AGW cases, the wake spectra exhibit a dominant peak at St  $\approx 0.3$ . Such a frequency peak arises from a convective shear-instability mechanism that dominates far-wake dynamics, which generates turbulent kinetic energy at 0.1 < St < 1. In the AGW case, the low-frequency inflow peaks (St  $\approx 0.05$  and St  $\approx 0.1$ ), shifts to a higher-frequency peak at St  $\approx 0.3$ at 4D downstream. This peak becomes less pronounced at 8D downstream as wake recovery weakens shear instabilities.



R-Fig. 5: Wake (solid lines) and inflow (dashed lines) spectra at downstream 4D (left) and 8D (right) from the single-turbine simulation.

Previous studies have shown that inflow velocity fluctuations at St < 0.3 directly drive wake meandering [5,6]. AGWs enhance inflow turbulent kinetic energy at St < 0.3, as shown by the dotted lines, and thus amplify wake meandering. This result is consistent with the work of Wise et al. [7], who reported that AGWs can increase turbulence levels and strengthen wake meandering.

The second and third highest St in the AGW wake spectra are approximately 0.44 and 0.66. The origin of these apparent harmonics is not unclear and will remain as a topic of future work.

## Revison

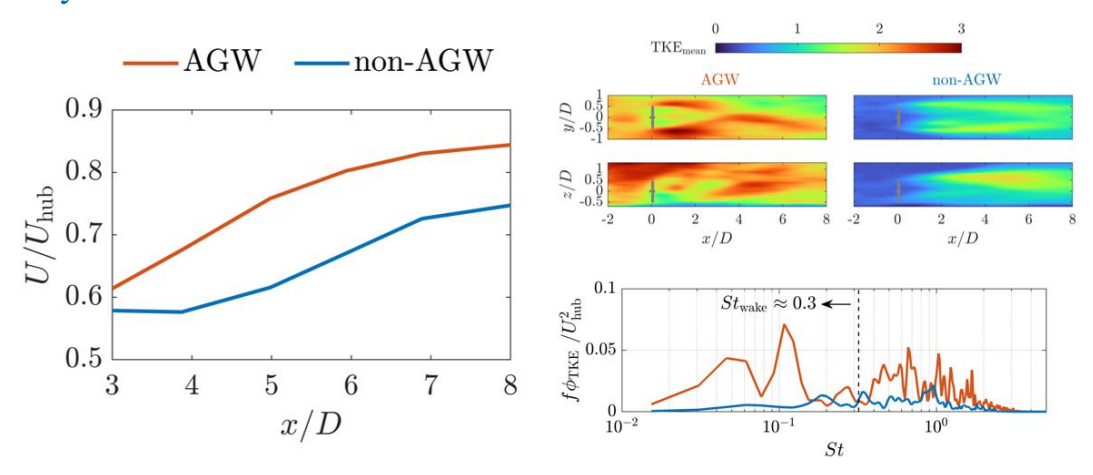
We have added 8D wake spectra from single-turbine simulation in Fig. 8 (as also shown in R-Fig. 5) and discussed the downstream evolution of wake spectra in lines 194-195.

'For both the AGW and non-AGW cases, such a frequency peak becomes less prominent in 8D downstream, because wake recovery has largely weakened shear instabilities at this region.'

(8) Wake velocity recovery. As noted on line 199 the distance to the maximum velocity deficit differs between the AGW and non-AGW cases. It is not however shown that the wake form is Gaussian at this point. The points on 'faster recovery of the mean wake of the AGW' should relate to the distances after this near-wake region. Over that range the AGW wake recovery is faster but it would be useful to bring out this rate of recovery of velocity more clearly. Differences of wake recovery are attributed to two mechanisms: i) stronger wake meandering due to larger-scale turbulent structures, and ii) higher value of TKE in the AGW case. The earlier sections should be modified to support these statements quantitatively including clarification of: the scales of turbulent structures in the onset flows, that the wake meandering is at the AGW periods, the value of TKE of the non-AGW onset flow.

### **Reply**

We agree with the reviewer's suggestion and have replotted Fig. 10 (also shown as the left panel of R-Fig. 6) to illustrate the rate of wake recovery in the far-wake region. The far wake is defined as the region where the spanwise wake profile becomes Gaussian. Based on the mean velocity contours in Fig. 9, we identify x/D > 3 as the far-wake region. In this region, the AGW case exhibits a higher recovery rate than the non-AGW case.



R-Fig. 6: Mean streamwise wake deficit along the turbine centerline (left). Wake TKE contours (top-right). Inflow spectra (bottom-right).

As discussed in the original draft, the faster wake recovery in the AGW case can be attributed to two factors: (i) enhanced wake meandering and (ii) higher turbulent kinetic energy. The first factor is supported by the meandering amplitudes shown in Fig. 5 and the inflow spectra in Fig. 8 (and in the bottom-right panel of R-Fig. 6). The increased inflow turbulent kinetic energy at St < 0.3 drives larger wake meandering amplitudes [5,6]. The second factor is supported by the mean turbulent kinetic energy contours in the top-right panel of R-Fig. 6, which show significantly higher levels in the AGW case compared with the non-AGW case.

### Revison

- (i) We have repotted Fig. 10 in the original draft with shorter streamwise extent, and rearranged it to make it the right panel of Fig. 7 in the revised draft.
- (ii) We have rewritten the discussion on the reasons for faster wake recovery in lines 220-224.

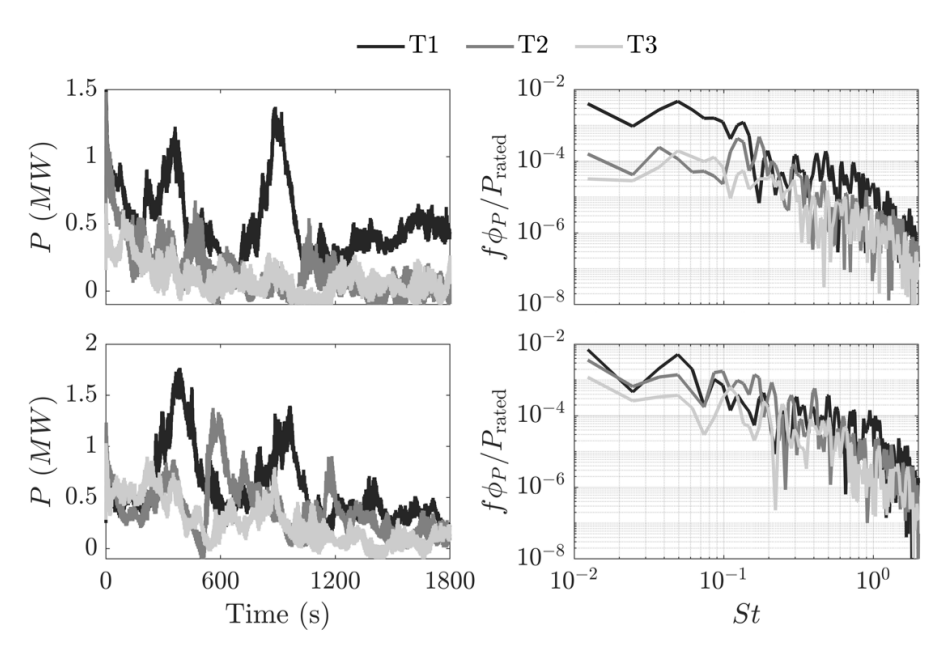
'The faster mean wake recovery in the AGW case can be attributed to two key factors: (i) Stronger wake meandering: The inflow spectra in Fig. 8 shows that the AGW inflow contains more intense large-scale turbulent structures, leading to greater meandering amplitudes and, consequently, larger mean wake expansion (Ainslie, 1988; Larsen et al., 2008). (ii) Higher turbulence levels: The mean turbulent kinetic energy contours in Fig. 6 show significantly higher turbulence levels in the AGW case. The increase of TKE enhances turbulent mixing, making the velocity recovery to be faster in the wake region.'

(9) Power attenuation is interesting to observe. However, this spacing is much closer than at the site or for any practical operating conditions so justification is required of the relevance of this layout. Some discussion is also needed on how these observed variations of power relate to the choice of turbine. At this spacing mean power on second turbine is about one-third of that on the leading turbine (hub height velocity is  $\sim 0.700$  as figure 8) so fluctuating load relative to the mean seems to increase with downstream rotor position (even though wake TKE similar to ambient TKE). Is the third turbine still within the operating range of the turbine if Uhub  $\sim 0.7 * 0.7 U0 \sim 2.5 \text{ m/s}$ ?

#### **Reply**

The reviewer is correct that the turbine spacing of 4D in our three-turbine simulation is smaller than the spacings typically used in operational wind farms. We intentionally adopted 4D spacing to ensure that the downstream turbines remain in the wake region of the upstream turbines, allowing their power outputs to serve as indicators of upstream wake characteristics.

To clarify this point, we performed an additional three-turbine simulation with 8D spacing. R-Fig. 7 shows the time series (left) and spectra (right) of turbine power for the 4D (top) and 8D (bottom) cases. For 4D spacing, AGWs induce large-scale power oscillations at the first turbine (T1), which are strongly attenuated at the downstream turbines (T2 and T3). For 8D spacing, the attenuation of power oscillations is weaker, and T2 still exhibits clear peaks with a time delay relative to T1. The difference in attenuation between the 4D and 8D cases is also evident in the spectra. This behavior arises because, as discussed in our reply to Comment 7, the shear instability mechanism that damps low-frequency velocity fluctuations becomes weaker farther downstream.



R-Fig. 7: Time series (left) and spectra (right) of turbine power for the three-turbine simulations with 4D (top) and 8D (bottom) spacings during the AGW event.

Regarding the reviewer's concern about the operating condition of T3, the time series of exact power (left panel of R-Fig. 7) confirms that T3 remains within its operating range for both 4D and 8D spacings. In our simulations, we set a constant rotational speed of 9 RPM. At low wind speeds, the aerodynamic torque is not enough to overcome generator and drivetrain losses. As a result, the reported power output can be negative, meaning the turbine is consuming electrical power to keep the generator running. We have modified Fig. 12 to the top panel in R-Fig. 7.

We agree with the reviewer that more realistic turbine layouts and more combinations of turbine spacing vs. AGW wavelength should be considered to fully understand the interactions between AGWs and wind farms. These topics will be pursued in future work.

# Revison

We have added the power outputs for the three-turbine simulation with an 8D spacing in Fig. 11 (as also shown in R-Fig. 5) and discussed the power attenuation in lines 230-235.

Figure 11 shows time series (left) and spectra (right) of turbine power for the three-turbine simulations with 4D (top) and 8D (bottom) spacings. For 4D spacing, the presence of AGWs induces large-scale power oscillations at the first turbine (T1), which are strongly attenuated at the downstream turbines (T2 and T3). For 8D spacing, the attenuation of power oscillations is weaker, and T2 still exhibits visible peaks with a time delay relative to T1. The difference in power attenuation between 4D and 8D spacing is also evident in the corresponding spectra. This behavior is because, as we showed in Fig. 8, the shear instability

mechanism that damps low-frequency velocity fluctuations becomes weaker at further downstream.'

# Reference

- [1] Allaerts, D., Quon, E., and Churchfield, M.: Using observational mean-flow data to drive large-eddy simulations of a diurnal cycle at the SWiFT site, Wind Energy, 26, 469 492, 2023.
- [2] Churchfield, M. J., Lee, S., Michalakes, J., and Moriarty, P. J.: A numerical study of the effects of atmospheric and wake turbulence on wind turbine dynamics, Journal of turbulence, p. N14, 2012.
- [3] Wu, Y.-T. and Porté-Agel, F., 2011. Large-eddy simulation of wind-turbine wakes: evaluation of turbine parametrisations, Boundary-layer meteorology,
- 138, pp.345 366.
- [4] Stevens, R.J., Martínez-Tossas, L.A. and Meneveau, C., 2018. Comparison of wind farm large eddy simulations using actuator disk and actuator line models with wind tunnel experiments. Renewable energy, 116, pp.470-478.
- [5] Larsen, G. C., Madsen, H. A., Thomsen, K., and Larsen, T. J., 2008. Wake meandering: a pragmatic approach, Wind Energy: An International Journal for Progress and Applications in Wind Power Conversion Technology, 11, pp.377–395.
- [6] Feng, D., Li, L. K., Gupta, V., and Wan, M., 2022. Componentwise influence of upstream turbulence on the far-wake dynamics of wind turbines, Renewable Energy, 200, pp.1081–1091.
- [7] Wise, A.S., Arthur, R.S., Abraham, A., Wharton, S., Krishnamurthy, R., Newsom, R., Hirth, B., Schroeder, J., Moriarty, P. and Chow, F.K., 2025. Large-eddy simulation of an atmospheric bore and associated gravity wave effects on wind farm performance in the southern Great Plains, Wind Energy Science, 10(6), pp.1007-1032.